The Impact of Electrogram Type and Conduction Velocity Estimation Techniques on Assessments of Conduction Velocity during Ventricular Substrate Mapping

Mahmoud Ehnesh[1], Johanna Tonko[2], Alexander M. Zolotarev[1], Edward J Vigmond[3], Pier D Lambiase[2] Caroline Roney[1]

[1]. Queen Mary University of London, UK
[2]. University College London, Institute for Cardiovascular Sciences, Centre for Translational Electrophysiology, UK
[3]. Université de Bordeaux, Institut de Mathématiques de Bordeaux, France

Abstract

Conduction velocity (CV) mapping has the potential to identify critical regions of the ventricular substrate to target by ablation. However, it is unknown how electrogram modality and methodology affects CV estimation. We aimed to test these effects in a control population for patients with structurally normal hearts and idiopathic ventricular ectopy.

Electroanatomical contact mapping was performed using EnSite™ X (Abbott) with the Advisor HD Grid for patients with structurally normal hearts undergoing elective ventricular ectopy ablation. CV was assessed using four methods: 1. omnipolar wavespeed (Abbott); 2. local gradient estimation from the interpolated LAT field; 3. fitting a planar wavefront to LAT measurements; 4. fitting a circular wavefront and estimating CV. CV estimates were compared between methods.

We analysed a total of 25 maps for 5 cases. Our results reveal than mean CV depends on CV estimation technique: e.g. for omnipolar recordings, wavespeed, Mean ± SD (m/s); 1.06 ±3.36; gradient;0.62 ±0.40; fitting a planar wavefront; 0.94 ±0.42; fitting a circular wavefront; 0.93 ±0.90. Median pointwise difference is also large between EGMs and across techniques.

Thus, in structurally normal hearts, CV estimation technique has a large effect on CV maps calculated during ventricular substrate mapping.

1 Introduction

Ventricular tachycardia (VT) is associated with significant morbidity and mortality [1]. Percutaneous catheter ablation has emerged as an important adjunctive therapy option for patients with idiopathic or scar related ventricular tachycardias [2]. The underlying electrophysiological substrate can be characterised using intracardiac electrograms (EGMs) [3]. Analysis of EGM features such as voltage, timing, morphology and functional characteristics of the electrical propagation, including conduction velocity (CV) estimation, offers valuable insights into the origin and underlying mechanism of the arrhythmia [3]. However, electro-anatomical maps obtained through unipolar or bipolar EGMs signals have intrinsic limitations, for example. signal morphology is inherently influenced by the relative orientation of the bipole to the direction of wavefront [4, 5]. To address these limitations, omnipolar mapping technology was developed, designed to extract maximal bipolar voltage independent of wavefront propagation direction and inform about directionality and speed of the wavefront. Importantly, omnipolar mapping offers estimates of wavefront speed that are orientation-independent, which can be compared to traditional local activation times (LAT) based CV techniques [6]. Regions of slow CV, often observed in surviving myocyte bundles within regions of scar, represent a functionally critical substrate for reentry VT, and targeting these areas during ablation procedures holds promise [7]. Fundamental to the characterisation of the substrate is the accurate calculation of cardiac CV. As automated CV algorithms become integrated into electroanatomic mapping system modules, discussions surrounding their accuracy and implications have been prevalent in recent literature [8, 9]. Various methods exist for calculating CV, each with its own advantages and disadvantages [9].

Understanding the influence of electrogram modality selection and CV estimation technique on CV maps is paramount. This study aims to investigate the effects of electrogram choice and CV methodology on CV estimation in a dataset of patients with structurally normal hearts and idiopathic ventricular ectopy.

2 Methods

2.1 Electrophysiological Study and Data Collection

Five patients with idiopathic ventricular ectopy and structurally normal hearts, as confirmed by cardiac magnetic resonance imaging (MRI), were retrospectively analysed for this study. All patients underwent elective ablation procedures as part of their routine clinical care. Electrophysiological mapping of the clinical ventricular ectopy was conducted using the EnSite™ mapping system with the Advisor HD Grid employing omnipolar technology. High density electroanatomic substrate and activation maps were created as per routine clinical care. EGMs, including omnipolar, bipolar, and unipolar recordings, were exported together with the anatomical mesh, electrode locations, LAT and wavefront speeds for offline postprocessing. Data was collected with approval of the local ethic committee. All patients provided written informed consent.

2.2 LAT Annotation

We developed automated algorithms to assign LAT to unipolar, bipolar and omnipolar signals using the steps outlined in this section. To compare between signal types, we assigned one unipolar LAT and one bipolar LAT to each set of signals comprising an omnipolar recording LAT. Specifically, we first annotated the LAT of each unipole among the three unipoles of EGMs, by identifying the timing of their steepest unipolar EGM slopes (maximum negative deflection - dV/dt). Then since each omnipolar signal is constructed using three unipolar signals in the across, along and corner orientations, we selected the LAT corresponding to the maximum of the three absolute slopes. For bipolar EGMs, the LAT of each bipole within the two available bipoles (across and along orientations) was similarly annotated, selecting the maximum absolute slope (maximum dV/dt). Once again, only the distal bipole displaying the maximum absolute slope was chosen. A similar approach was adopted for omnipolar EGMs, where the maximum absolute slope (maximum deflection dV/dt) was used for LAT annotation. Subsequently, all LAT values for EGMs were interpolated onto a 2mm resolution mesh using inverse distance weighting interpolation.

2.3 Calculation of Conduction Velocity (CV).

CV was assessed through four distinct methods:

- Omnipolar wavespeed derived from the EnSite™ mapping system.
  - Local gradient estimation based on the interpolated LAT field.
  - Fitting a planar wavefront to LAT measurements within a 6mm radius of each recording location.
  - Fitting a circular wavefront and estimating its CV.

2.3.1 Estimation of wavespeeds with Omnipolar method.

As described by Deno et al. (2017) [6], omnipolar wavespeeds were determined by assuming a planar and homogeneous wave within a group of nearby electrodes referred to as a 'clique.' This method is based on the relationship between the spatial gradient of unipolar voltage and the electric field at the extracellular-myocardial interface. It involves estimating the electric field at the centre of a clique consisting of three or more electrodes using a least-squares fit, and then it identifies the direction that maximizes the cross-correlation between the first temporal derivative of the unipolar voltage and the multiple bipole derived electric field in that particular direction. The wavespeed is estimated by calculating the ratio of amplitudes of the first temporal derivative of the unipolar voltage to the omnipolar field component along the activation direction without the need for prior estimation of LAT [10, 11].

2.3.2 Estimation of CV methods based on LAT calculation.

In the local LAT gradient technique, CV estimation relies on the spatial gradients of LAT. This involves deriving the spatial gradient of LAT, often referred to as the 'slowness' vector ($\nabla T(x)$), which can be derived and inverted to calculate CV using the formula in equation (1). The values of the slowness vector for each mesh element can be determined using piecewise linear functions [9].

$$CV = \frac{\nabla T(x)}{|\nabla T(x)|^2} \qquad (01)$$

For cosine-fit techniques, a previously published automated method has been employed for CV estimation [8]. This technique assumes either planar or circular wavefront propagation and utilises a cosine-fit algorithm with a constant velocity. It is adaptable for different wavefront types and any arrangement of points on a curved surface, ultimately generating a spatial map depicting the velocity of wavefront propagation, assuming either planar or circular wavefront propagation.

In the case of the planar technique, it assumes a planar wavefront propagation inside a circle of radius r with waves passing over a circle of recording points characterised by a constant offset γ and a radius of curvature r

$$t_{(n)} = t_C - A\cos\,[\gamma(n-1) - \emptyset_0] \qquad (02)$$

The activation time centre t_C and the angle of earliest activation $\emptyset_0$, thus unknowns t_C, A and $\emptyset_0$, could be initially estimated based on the sequence of activation. These parameters are then fit using least squares fitting, and CV is then determined.

CV estimates were compared both within different methods and among the various types of EGMs.

3 Statistical Analysis

The statistical analysis was performed using GraphPad Prism (version 7.04 for Windows). Continuous variables with a normal distribution were represented as mean values (± standard deviation). To assess the variations in CV values among different EGMs types for each technique, we performed an ordinary one-way analysis of variance (ANOVA), $p < 0.05$ was considered statistically significant.

4 Results

We analysed a total of 25 maps across five patients. An example is shown in Figure 1.

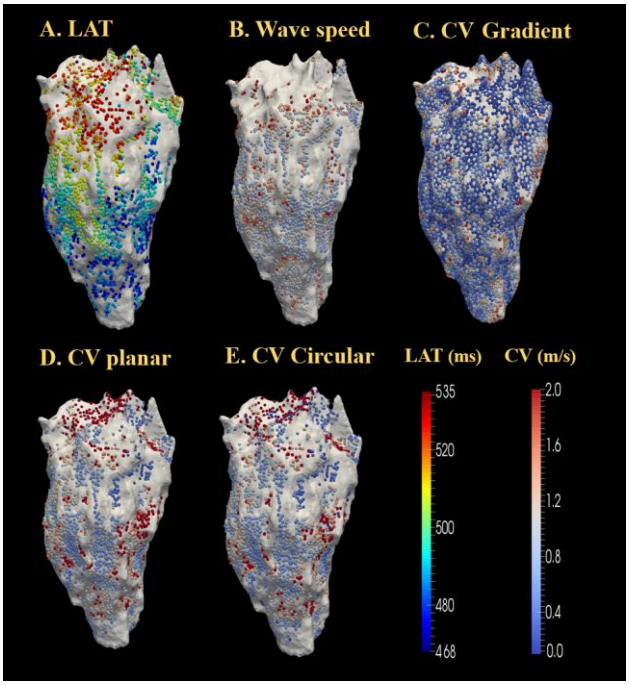

Figure 1. The 3D representation of a patient's left ventricle in sinus rhythm. A. LAT map. B. Wave speed of omnipolar recordings using Ensite system. C. CV derived from local LAT gradient. D. CV using planar wavefront fitting E. CV using circular wavefront fitting. The colour bars show LAT in milliseconds and CV in meters per second across various regions on the 3D left atrial geometry for both LAT and CV techniques.

Figure 2 shows the mean CV values for each technique across different types of EGMs. For the gradient, the mean CV (measured in meters per second), along with their respective standard deviations (±SD) were as follows: omnipolar 0.62 ± 0.40, bipolar 0.62 ± 0.41, and unipolar 0.66 ± 0.41. In the case of fitting a planar wavefront, the mean of the CV were as follows: omnipolar 0.92 ± 0.40, bipolar 0.90 ± 0.40, and unipolar 0.99 ± 0.45. Similarly, for fitting a circular wavefront, the mean CV values were recorded as follows: omnipolar 0.91 ± 1.09, bipolar 0.90 ± 0.58, and unipolar 1.01 ± 0.74.

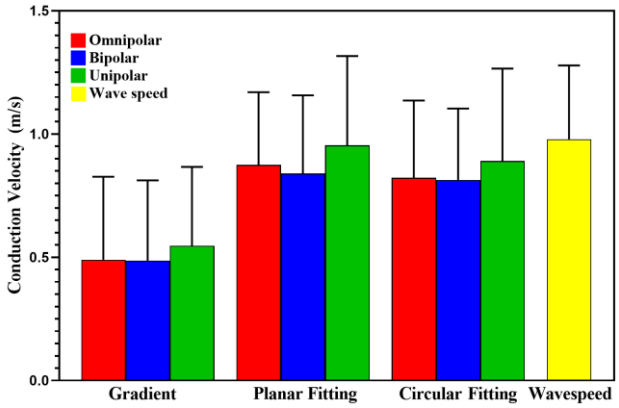

Figure 2. The comparison between EGMs types and CV estimation techniques is represented by the mean ± SD for each CV technique within the specific EGMs type.

We identified a significant median pointwise difference among EGM types and across different techniques. Specifically, for omnipolar EGM, the median pointwise variations are as follows: wavespeed vs gradient: 0.51 m/s, wavespeed vs fitting a planar wavefront: 0.37 m/s, and gradient vs fitting a planar wavefront: 0.43 m/s. Likewise, within bipolar EGM, the median pointwise disparities are outlined as follows: wavespeed vs gradient: 0.51 m/s, wavespeed vs fitting a planar wavefront: 0.39 m/s, and gradient vs fitting a planar wavefront: 0.44 m/s. Lastly, in the unipolar EGM, the median pointwise discrepancies are documented as follows: wavespeed vs gradient: 0.46 m/s, wavespeed vs fitting a planar wavefront: 0.39 m/s, and gradient vs fitting a planar wavefront: 0.46 m/s (see Figure 3).

In Figure 3, the wavespeed values imported from the EnSite X system were utilised for comparative analysis with bipolar and unipolar EGMs, while other CV estimation methods were individually calculated for each EGM type.

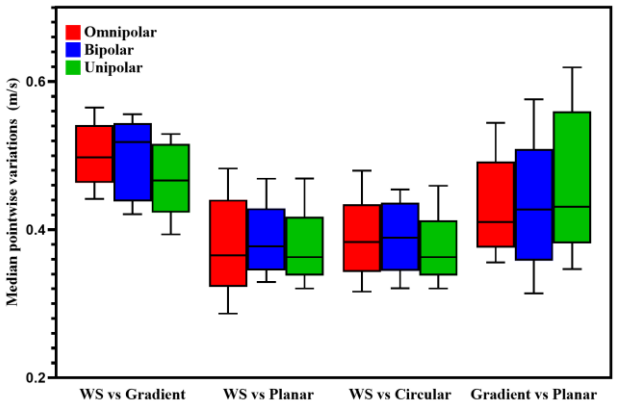

Figure 3. Pointwise differences among EGM types and across various CV estimation techniques. WS (wavespeed), Gradient (local LAT gradient CV), Planar (planar wavefront fitting), and Circular (circular wavefront fitting).

5 Discussion

Regions with slow conduction in SR may be predictive of VT termination sites [12]. Here, we use SR data of patients with structurally normal heart for an initial comparison of CV estimation algorithms to establish references values that can be considered normal in healthy tissue for the respective methodology. Our results show that the choice of CV techniques during SR mapping affect CV values. Knowledge about these quantitative differences between CV estimation methods is important to inform the choice of method for substrate mapping in structurally abnormal hearts to identify zones of abnormal slowing. The variation in the CV results among the selected techniques shown in Figure 1 (B, C, D, and E) may be due to interpolation, averaging, and the locality of the CV estimation [13]. For instance, different interpolation methods yield perceived differences in LAT maps [14]. The gradient method estimates CV over a small area of the mesh (a single element), so it provides a local measurement and can detect areas of CV heterogeneity; however, it is dependent on LAT interpolation, so more prone to error. Wavefront fitting techniques calculate CV over a larger area and do not require interpolation so are less sensitive to noise but may not capture all CV heterogeneity. In forthcoming research, there will be an evaluation of the potential integration of uncertainty quantification methodologies, either within the process of LAT assignment or CV estimation techniques [9]. This endeavor aims to provide valuable insights to mitigate the variability observed in the results of CV estimation techniques.

6 Conclusion

In patients with structurally normal hearts undergoing electrophysiological procedures, CV estimation technique has a large effect on SR CV maps calculated during ventricular substrate mapping.

Acknowledgments

Dr Caroline Roney acknowledges support from a UKRI Future Leaders Fellowship (MR/W004720/1).

References

[1] A. Kumar, D. M. Avishay, C. R. Jones, J. D. Shaikh, R. Kaur, M. Aljadah, A. Kichloo, N. Shiwalkar, and S. Keshavamurthy, "Sudden Cardiac Death: Epidemiology, Pathogenesis and Management," *Reviews in Cardiovascular Medicine*, vol. 22, no. 1, pp. 147-158, 2021.

[2] C. W. Tsao, A. W. Aday, Z. I. Almarzooq, A. Alonso, A. Z. Beaton, M. S. Bittencourt, A. K. Boehme, A. E. Buxton, A. P. Carson, and Y. Commodore-Mensah, "Heart Disease and Stroke Statistics—2022 update: a report from the American Heart Association," *Circulation*, vol. 145, no. 8, pp. e153-e639, 2022.

[3] B. Berte, K. Zeppenfeld, and R. Tung, "Impact Of Micro-, Mini-And Multi-Electrode Mapping On Ventricular Substrate Characterisation," *Arrhythmia & electrophysiology review*, vol. 9, no. 3, pp. 128, 2020.

[4] M. S. van Schie, R. K. Kharbanda, C. A. Houck, E. A. Lanters, Y. J. Taverne, A. J. Bogers, and N. M. de Groot, "Identification of Low-Voltage Areas: A Unipolar, Bipolar, and Omnipolar Perspective," *Circulation: Arrhythmia and Electrophysiology*, vol. 14, no. 7, pp. e009912, 2021.

[5] M. Takigawa, J. Relan, R. Martin, S. Kim, T. Kitamura, A. Frontera, G. Cheniti, K. Vlachos, G. Massoullié, and C. A. Martin, "Effect of Bipolar Electrode Orientation on Local Electrogram Properties," *Heart Rhythm*, vol. 15, no. 12, pp. 1853-1861, 2018.

[6] D. C. Deno, R. Balachandran, D. Morgan, F. Ahmad, S. Massé, and K. Nanthakumar, "Orientation-Independent Catheter-Based Characterization of Myocardial Activation," *IEEE transactions on biomedical engineering*, vol. 64, no. 5, pp. 1067-1077, 2017.

[7] C. B. Brunckhorst, W. G. Stevenson, K. Soejima, W. H. Maisel, E. Delacretaz, P. L. Friedman, and S. A. Ben-Haim, "Relationship of Slow Conduction Detected By Pace-Mapping To Ventricular Tachycardia Re-Entry Circuit Sites After Infarction," *Journal of the American College of Cardiology*, vol. 41, no. 5, pp. 802-809, 2003.

[8] C. D. Cantwell, C. H. Roney, F. S. Ng, J. H. Siggers, S. J. Sherwin, and N. S. Peters, "Techniques For Automated Local Activation Time Annotation And Conduction Velocity Estimation In Cardiac Mapping," *Computers in biology and medicine*, vol. 65, pp. 229-242, 2015.

[9] S. Coveney, C. Cantwell, and C. Roney, "Atrial Conduction Velocity Mapping: Clinical Tools, Algorithms And Approaches For Understanding The Arrhythmogenic Substrate," *Medical & Biological Engineering & Computing*, vol. 60, no. 9, pp. 2463-2478, 2022.

[10] J. Riccio, A. Alcaine, S. Rocher, L. Martinez-Mateu, S. Laranjo, J. Saiz, P. Laguna, and J. P. Martínez, "Characterization Of Atrial Propagation Patterns And Fibrotic Substrate With A Modified Omnipolar Electrogram Strategy In Multi-Electrode Arrays," *Frontiers in Physiology*, vol. 12, pp. 674223, 2021.

[11] J. Riccio, A. Alcaine, N. M. de Groot, R. Houben, P. Laguna, and J. P. Martínez, "Characterization Of Propagation Patterns With Omnipolar EGM In Epicardial Multi-Electrode Arrays." 1-4 Computing in Cardiology 2019; Vol 46 Page 2 ISSN: 2325-887X DOI: 10.22489/CinC.2019.340.

[12] E. Anter, A. G. Kleber, M. Rottmann, E. Leshem, M. Barkagan, C. M. Tschabrunn, F. M. Contreras-Valdes, and A. E. Buxton, "Infarct-Related Ventricular Tachycardia: Redefining The Electrophysiological Substrate Of The Isthmus During Sinus Rhythm," *JACC: Clinical Electrophysiology*, vol. 4, no. 8, pp. 1033-1048, 2018.

[13] C. H. Roney, J. Whitaker, I. Sim, L. O'Neill, R. K. Mukherjee, O. Razeghi, E. J. Vigmond, M. Wright, M. D. O'Neill, and S. E. Williams, "A Technique For Measuring Anisotropy In Atrial Conduction To Estimate Conduction Velocity And Atrial Fibre Direction," *Computers in biology and medicine*, vol. 104, pp. 278-290, 2019.

[14] J. Hellar, R. Cosentino, M. M. John, A. Post, S. Buchan, M. Razavi, and B. Aazhang, "Manifold Approximating Graph Interpolation of Cardiac Local Activation Time," *IEEE Transactions on Biomedical Engineering*, vol. 69, no. 10, pp. 3253-3264, 2022.

Address for correspondence:
Mahmoud Ehnesh
Postal address: 67-75 New Road, London E1 1HH
E-mail. **m.ehnesh@qmul.ac.uk**